

Investigation on polycrystallization mechanism at initial interfaces in $\text{In}_x\text{Ga}_{1-x}\text{As}$ ($x \sim 0.3$) bulk crystals on lattice mismatched seeds

By

Hiroaki MIYATA^{2,3}, Yasuyuki OGATA¹, Satoshi ADACHI¹, Tetsuya TSURU²,
Yuji MURAMATSU², Kyoichi KINOSHITA¹, Osamu ODAWARA³ and Sinichi YODA^{1,3}

Abstract : In the growth of $\text{In}_{0.3}\text{Ga}_{0.7}\text{As}$ single crystals, polycrystallization at the initial interface with lattice-mismatched seeds is a major problem because no homogeneous $\text{In}_{0.3}\text{Ga}_{0.7}\text{As}$ seed crystals have been obtained and usually GaAs crystals are used as seeds. Hence, a mechanism of polycrystallization at the initial interface was investigated. In this paper, a local misfit stress at the interface is calculated. Then it is compared with the critical resolved shear stress (CRSS). It was determined that the polycrystallization at the initial interface is related to the magnitude of the misfit stress and to that of the CRSS. We discuss growth of larger $\text{In}_{0.3}\text{Ga}_{0.7}\text{As}$ single crystals by avoiding the polycrystallization at the initial interface.

Key words : Single crystal growth, Growth from solutions, Gallium compounds, Semiconduction ternary compounds

1. Introduction

An $\text{In}_{0.3}\text{Ga}_{0.7}\text{As}$ bulk crystal is expected to be a next generation substrate suitable for optoelectronics devices such as a laser diode at 1.3 μm wavelength [1]. However, polycrystallization at the initial interface has occurred because of a misfit between a grown crystal and a seed, as shown in Fig. 1. Therefore, large-sized $\text{In}_{0.3}\text{Ga}_{0.7}\text{As}$ single crystals, which are applicable to devices, have not been obtained. Many investigations have been conducted on thin films to try to resolve the polycrystallization by misfit [2-5]. However, the theory about thin films cannot be directly applied to bulk crystal growth from melts. Hence, a new model is required for bulk crystal growth. Figure 2 shows observed images of the initial interface, whose combinations of a seed and a grown crystal are different. Photograph (a) is the combination of $\text{In}_{0.05}\text{Ga}_{0.95}\text{As}$ seed / $\text{In}_{0.3}\text{Ga}_{0.7}\text{As}$ ($f=1.78\%$), (b) GaAs seed / $\text{In}_{0.2}\text{Ga}_{0.8}\text{As}$ ($f=1.43\%$), (c) GaAs seed / $\text{In}_{0.15}\text{Ga}_{0.85}\text{As}$ ($f=1.08\%$) and (d) GaAs seed / $\text{In}_{0.09}\text{Ga}_{0.91}\text{As}$ ($f=0.64\%$), respectively. The misfit is smallest at the combination (d). As shown in these photographs, the larger the misfit, the more significant the polycrystallization at the initial interface is. In our experiments, the threshold for taking over is $f=0.6\text{-}0.7\%$, in the case of GaAs seeds. So it is difficult to grow $\text{In}_{0.3}\text{Ga}_{0.7}\text{As}$ single crystals without lattice matched seeds. However, an allowance of misfit in the bulk crystals growth is considerably larger compared with thin films, whose critical thickness is only several tens micro meter in the case of $f \sim 0.6\%$ [5]. This is attributed to the fact that the concentration gradient layer (Fig. 3), which is formed at the initial

¹The Institute of Space and Astronautical Science (ISAS)/JAXA

²Advanced Engineering Services Co., Ltd.

³Tokyo Institute of Technology

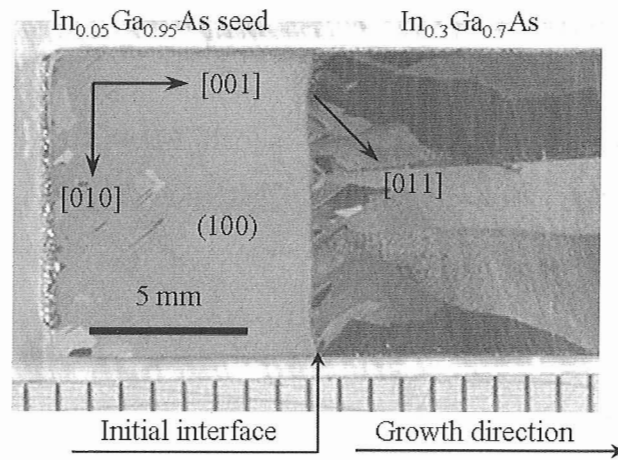


Fig. 1 Roughly polished surface of the initial interface of an $\text{In}_{0.3}\text{Ga}_{0.7}\text{As}$ crystal grown on an $\text{In}_{0.05}\text{Ga}_{0.95}\text{As}$ seed.

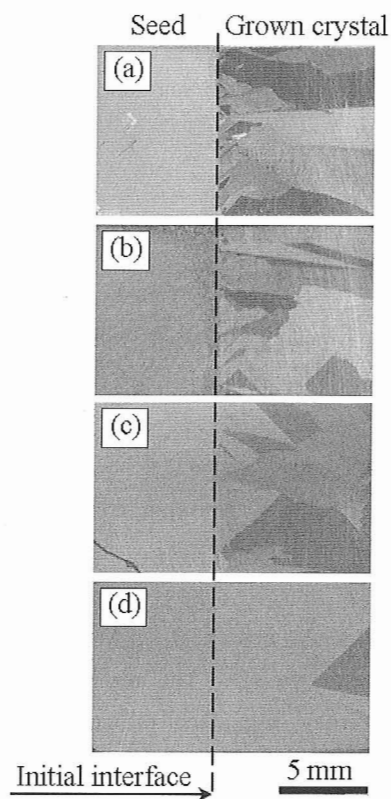


Fig. 2 Roughly polished surface of the initial interfaces, combinations of a seed and a grown crystal are (a) $\text{In}_{0.05}\text{Ga}_{0.95} / \text{In}_{0.3}\text{Ga}_{0.7}\text{As}$, (b) $\text{GaAs} / \text{In}_{0.2}\text{Ga}_{0.8}\text{As}$, (c) $\text{GaAs} / \text{In}_{0.15}\text{Ga}_{0.85}\text{As}$ and (d) $\text{GaAs} / \text{In}_{0.09}\text{Ga}_{0.91}\text{As}$.

interface in the bulk crystals growth from melts, disperses a misfit. We focused on this gradient layer. On the other hand, based on the observation of the initial interface, we assumed that a misfit stress causes slip, and this triggers the polycrystallization. To confirm this hypothesis, we calculated a local misfit stress (LMS) at the gradient layer. Then the calculated LMS was compared with the critical resolved shear stress (CRSS). In addition, we discussed growth of larger $\text{In}_{0.3}\text{Ga}_{0.7}\text{As}$ single crystals based on the analysis.

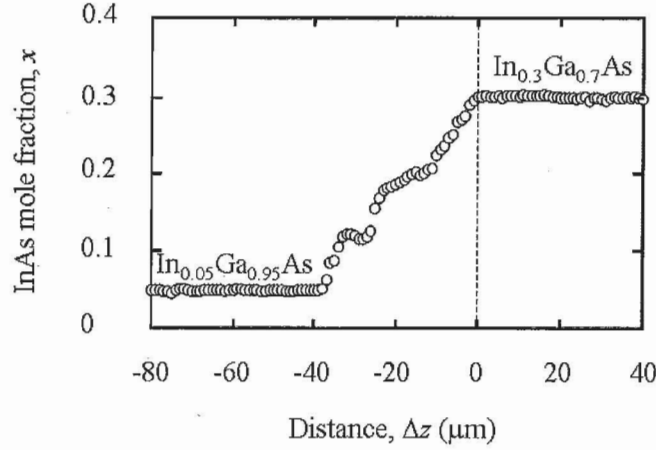


Fig. 3 Result of EPMA measurement of the initial interface of $\text{In}_{0.3}\text{Ga}_{0.7}\text{As}$ growth on an $\text{In}_{0.05}\text{Ga}_{0.95}\text{As}$ seed.

2. Model

As mentioned, the concentration gradient layers are formed at the initial interface. This model assumes that unit cells are loaded on a seed with increasing their InAs mole fraction in accordance with the growth (Fig. 4 (a)). The calculation is made for a shear stress on the hatched unit cell in Fig. 4 (a), of which the temperature is assumed to be ΔT lower than the freezing interface. This means that the cells begin to behave as elastic bodies at that temperature. Hence, the cells between the freezing interface and the hatched cell are stress-free, and the hatched cell receives compression stress (σ) by the constraint of seed side cells. However, for simplicity of the model, ΔT is considered as negligible in the calculation, because it makes only an infinitesimal difference to the results. As shown in Fig. 4 (b), the shear stress of a slip direction $\langle 110 \rangle$ on the slip plane $\{111\}$ is defined as a LMS (τ_l), and is calculated as below. Firstly, the lattice constant is obtained by the following equation (Vegard's law) from InAs mole fraction (x).

$$f(x) = 0.0404x + 0.5653 \quad [\text{nm}] \quad (1)$$

Because x is expressed as a function of the distance along the growth direction, Δz_n , in Eq. (1), $f(x)$ is rewritten as $g(\Delta z_n)$. Because the cells are assumed to be elastic bodies, generated stress is described as Eq. (2) (Hooke's law).

$$\begin{bmatrix} \sigma_X \\ \sigma_Y \\ \sigma_Z \\ \tau_{YZ} \\ \tau_{ZX} \\ \tau_{XY} \end{bmatrix} = \begin{bmatrix} c_{11} & c_{12} & c_{13} & c_{14} & c_{15} & c_{16} \\ c_{21} & c_{22} & c_{23} & c_{24} & c_{25} & c_{26} \\ c_{31} & c_{32} & c_{33} & c_{34} & c_{35} & c_{36} \\ c_{41} & c_{42} & c_{43} & c_{44} & c_{45} & c_{46} \\ c_{51} & c_{52} & c_{53} & c_{54} & c_{55} & c_{56} \\ c_{61} & c_{62} & c_{63} & c_{64} & c_{65} & c_{66} \end{bmatrix} \begin{bmatrix} \varepsilon_X \\ \varepsilon_Y \\ \varepsilon_Z \\ \gamma_{YZ} \\ \gamma_{ZX} \\ \gamma_{XY} \end{bmatrix} \quad (2)$$

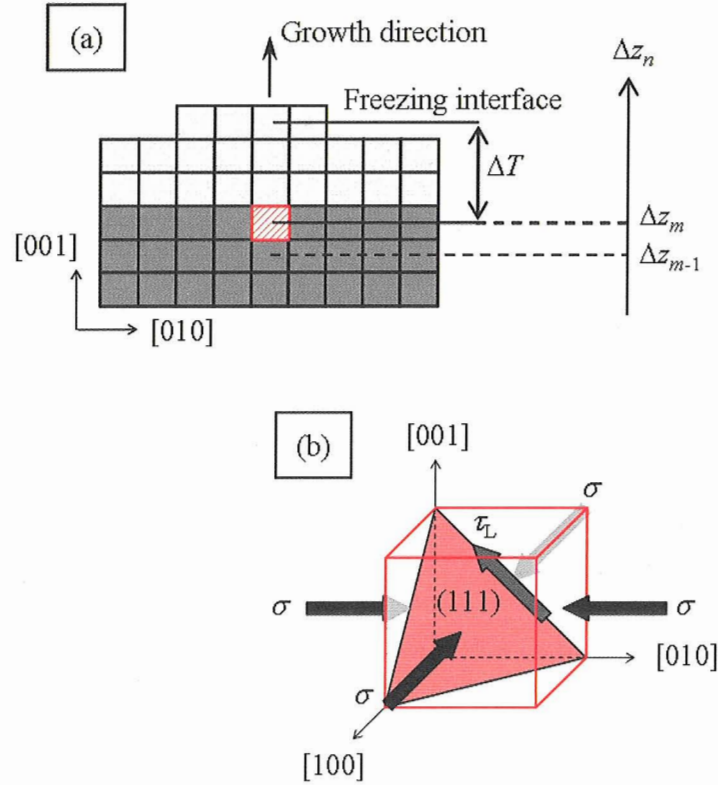


Fig. 4 Schematic diagram of a growth model, (a) a two-dimensional growth model, the hatched cell being subjected to calculation, (b) close-up of a unit cell corresponding to the hatched cell in (a).

where c is an elastic stiffness, ε is a normal strain and γ is a shear strain. In consideration of the strain orientation and the condition $\sigma_Z = \tau_{YZ} = \tau_{ZX} = \tau_{XY} = 0$, the Eq. (2) is rewritten as Eq. (3).

$$\begin{bmatrix} \sigma_X \\ \sigma_Y \\ 0 \\ 0 \\ 0 \\ 0 \end{bmatrix} = \begin{bmatrix} c_{11} & c_{12} & c_{12} & 0 & 0 & 0 \\ c_{12} & c_{11} & c_{12} & 0 & 0 & 0 \\ c_{12} & c_{12} & c_{11} & 0 & 0 & 0 \\ 0 & 0 & 0 & c_{44} & 0 & 0 \\ 0 & 0 & 0 & 0 & c_{44} & 0 \\ 0 & 0 & 0 & 0 & 0 & c_{44} \end{bmatrix} \begin{bmatrix} \varepsilon_X \\ \varepsilon_Y \\ \varepsilon_Z \\ \gamma_{YZ} \\ \gamma_{ZX} \\ \gamma_{XY} \end{bmatrix} \quad (3)$$

By substituting $\sigma_X = \sigma_Y = \sigma$ and $\varepsilon_X = \varepsilon_Y = \varepsilon$, loaded stress can be solved as follows,

$$\sigma = \frac{c_{11}^2 + 2c_{11}c_{12}}{c_{11} + c_{12}} \varepsilon \quad (4)$$

The ε can be obtained from the difference of lattice parameters of adjacent m th and $m-1$ th cells,

$$\varepsilon = \frac{g(\Delta Z_{m-1}) - g(\Delta Z_m)}{g(\Delta Z_m)} \quad (5)$$

Between the shear stress (τ) and the σ , there is a relationship described as Eq. (6) (Shmid's law).

$$\tau = \sigma \cos \phi \cos \lambda \quad (6)$$

where ϕ is an angle formed between stress axis $\langle 100 \rangle$ and normal line of slip plane $\langle 111 \rangle$ and λ is an angle formed between stress axis and slip direction $\langle 110 \rangle$. From Eq. (4), (5) and (6), the τ_L is obtained as Eq. (7):

$$\tau_L = \frac{c_{11}^2 + 2c_{11}c_{12}}{c_{11} + c_{12}} \frac{g(\Delta Z_{m-1}) - g(\Delta Z_m)}{g(\Delta Z_m)} \cos \phi \cos \lambda \quad (7)$$

The c_{11} and the c_{12} are functions of x and temperature (T). T is close to the temperature of the freezing interface (T_s). The c_{ij} of GaAs ($c_{ij, \text{GaAs}}$) at T_s are obtained by extrapolating the temperature dependence of elastic stiffness in GaAs [6]. The c_{ij} of InAs ($c_{ij, \text{InAs}}$) at T_s are obtained by the relationship between the c_{ij} of GaAs and InAs [7]. From these values, c_{ij} of $\text{In}_x\text{Ga}_{1-x}\text{As}$ are estimated as follows,

$$c_{ij} = xc_{ij, \text{InAs}} + (1-x)c_{ij, \text{GaAs}} \quad (8)$$

Strictly, the lattice constants must include the thermal expansion and its composition dependence. However, even if they were considered, differences would be less than 0.005 % in the calculation. So they are assumed negligible for simplicity of the model.

3. Results and Discussion

The calculated result of the misfit stress is shown in Fig. 5. The horizontal axes of three diagrams in the figure are all coincided. The upper diagram is a back-scattered electron microscope image of the initial interface, and it corresponds to the crystal of Fig. 1. The middle diagram shows a result of electron probe microanalyzer (EPMA) measurement and a best fitted line of them. The lower diagram shows the relationship between the τ_L and the CRSS of $\text{In}_x\text{Ga}_{1-x}\text{As}$ ($\tau_{c,x}$). The $\tau_{c,x}$ is a function of T and x , and is estimated by the following equation.

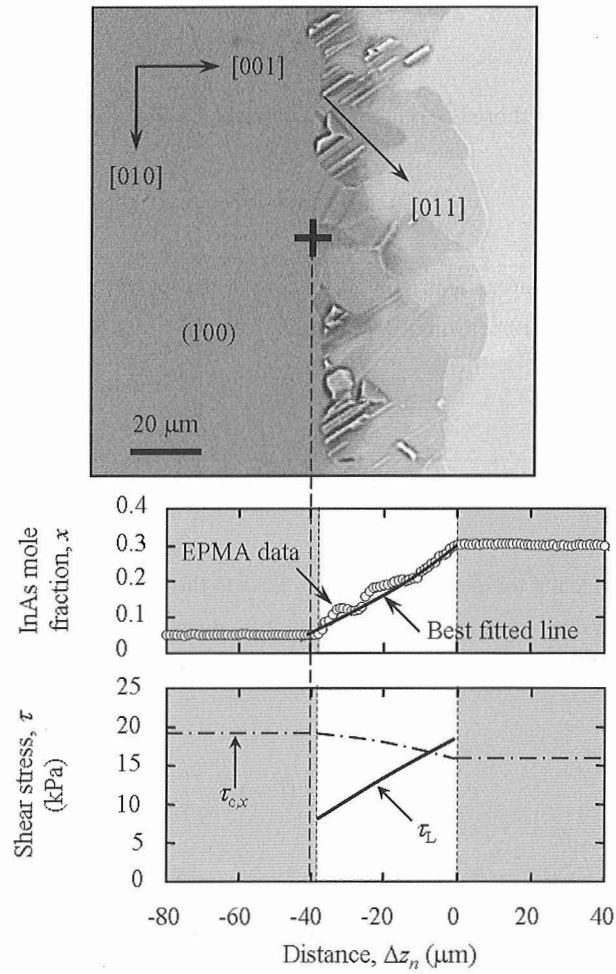


Fig. 5 Results of a back-scattered electron microscope image, EPMA measurement and local misfit analysis in $\text{In}_{0.3}\text{Ga}_{0.7}\text{As}$ growth on an $\text{In}_{0.05}\text{Ga}_{0.95}\text{As}$ seed.

$$\tau_{c,x} = x\tau_{c,\text{InAs}} + (1-x)\tau_{c,\text{GaAs}} \quad (9)$$

where $\tau_{c,\text{InAs}}$ and $\tau_{c,\text{GaAs}}$ are the CRSS of InAs and GaAs, respectively. These values are obtained by extrapolating the temperature dependence of CRSS in GaAs [8] and using the relationship between temperature dependence of yield stress in GaAs [9] and InAs [10]. From the lower diagram in Fig. 5, it is found that the τ_L is greater than the $\tau_{c,x}$ in the white region. In this case, slips are introduced, and this result agrees with the observed result as shown in the upper diagram. Such slips induce 60° dislocations and they cause polycrystallization because of the rotation of crystal orientations (Fig. 6). The left illustration shows a relationship between one regular octahedron in the zinc blende structure and a 60° dislocation, and the right illustration shows a tetragonal dodecahedron after running through the 60° dislocation.

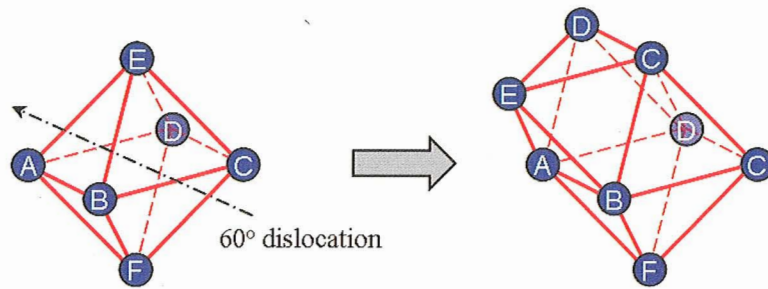


Fig. 6 Schematic diagram of rotation of crystal orientation by inducing 60° dislocation.

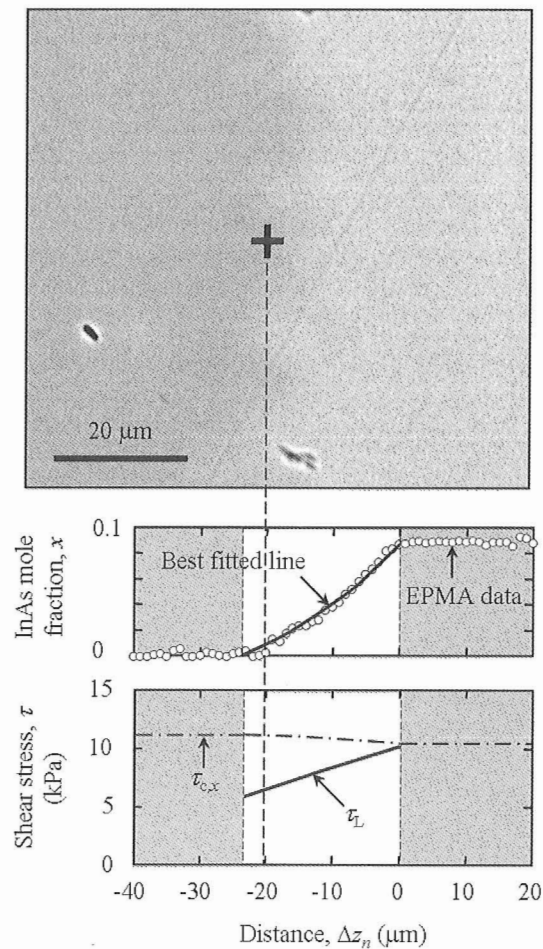


Fig. 7 Results of a back-scattered electron microscope image, EPMA measurement and local misfit analysis in $\text{In}_{0.09}\text{Ga}_{0.91}\text{As}$ growth on a GaAs seed.

On the other hand, in the case of the $\text{In}_{0.09}\text{Ga}_{0.91}\text{As}$ growth on the GaAs seed, grown crystals take over the orientation of seeds, according to our experimental results. For this GaAs / $\text{In}_{0.09}\text{Ga}_{0.91}\text{As}$ growth, the LMS analysis was applied. The result is shown in Fig. 7. From the lower diagram of this figure, it is found that the τ_L is less than the $\tau_{c,x}$ in all part of the white region. In this case, slips did not occur at the initial interface, as shown in the upper diagram of Fig. 7. These calculated results include a slight inaccuracy in the implication where complex mechanical properties of alloys were

simplified by the relationships such as Eq. (8) and (9). However, combined with the observation results, a large part of the mechanism of polycrystallization at the initial interface can be accounted for by the relation between the magnitude of τ_L and that of $\tau_{c,x}$. These results show that $\text{In}_{0.3}\text{Ga}_{0.7}\text{As}$ single crystal growth on lattice mismatched seeds can be achieved by gradual increase in the InAs mole fraction at the initial interface while retaining $\tau_L < \tau_{c,x}$.

4. Conclusions

To investigate the polycrystallization mechanism at the initial interface in InGaAs bulk crystals on lattice mismatched seeds, the local misfit stress (LMS) was calculated. In the case of $\text{In}_{0.3}\text{Ga}_{0.7}\text{As}$ growth on an $\text{In}_{0.05}\text{Ga}_{0.95}\text{As}$ seed, the LMS was greater than the critical resolved shear stress (CRSS) at the initial interface. On the other hand, in the case of $\text{In}_{0.09}\text{Ga}_{0.91}\text{As}$ growth on a GaAs seed, which successfully grows in a single crystal, the LMS was smaller than the CRSS. These results show that the large part of the mechanism of polycrystallization at the initial interface can be accounted for by the relation between the magnitude of the LMS and that of the CRSS. These results suggest that $\text{In}_{0.3}\text{Ga}_{0.7}\text{As}$ single crystals can be grown by keeping the LMS smaller than the CRSS at the initial interface.

References

- [1] H. Ishikawa, "Theoretical gain of strained quantum well grown on a ternary substrate", *Appl. Phys. Lett.*, 63, 712 (1993).
- [2] J.W. Matthews, A.E. Blakeslee, "Defects in epitaxial multilayers: I. Misfit dislocations", *J. Crystal Growth*, 27, 118 (1974).
- [3] J.W. Matthews, A.E. Blakeslee, "Defects in epitaxial multilayers: II. Dislocation pile-ups, threading dislocations, slip lines and cracks", *J. Crystal Growth*, 29, 273 (1975).
- [4] J.W. Matthews, A.E. Blakeslee, "Defects in epitaxial multilayers: III. Preparation of almost perfect multilayers", *J. Crystal Growth*, 32, 265 (1976).
- [5] R. People, J.C. Bean, "Calculation of critical layer thickness versus lattice mismatch for $\text{Ge}_x\text{Si}_{1-x}$ / Si strained-layer heterostructures", *Appl. Phys. Lett.*, 47 (3), 322 (1985).
- [6] Yu.A. Burenkov, Yu.M. Burenkov, S.Yu. Davidov, S.P. Nikanorov, "Temperature dependences of the elastic constants of gallium arsenide", *Soviet Phys-Solid State*, 15, 1175 (1973).
- [7] A. de Bernabe, C. Prieto, L. Gonzalez, Y. Gonzalez, A.G. Every, "Elastic constants of $\text{In}_x\text{Ga}_{1-x}\text{As}$ and $\text{In}_x\text{Ga}_{1-x}\text{P}$ determined using surface acoustic waves", *J. Phys.: Condens. Matter*, 11, 323 (1999).
- [8] T. Suzuki, T. Yasutomi, T. Tokuoka, "Plastic deformation of GaAs at low temperatures", *Philosophical Magazine*, A 79, 2637 (1999).
- [9] I. Yonenaga, U. Onose, K. Sumino, "Mechanical properties of GaAs crystals", *J. Mater. Res.* 2, 252 (1987).
- [10] I. Yonenaga, K. Sumino, "Mechanical properties and dislocation dynamics of III-V compound semiconductors", *Phys. Status Solidi a* 131, 663 (1992).